Journal of
Applied Remote Sensing

Intercomparison in the field between the new WISP-3 and other radiometers (TriOS Ramses, ASD FieldSpec, and TACCS)

Annelies Hommersom
Susanne Kratzer
Marnix Laanen
Ilmar Ansko
Martin Ligi
Mariano Bresciani
Claudia Giardino
José M. Beltrán-Abaunza
Gerald Moore
Marcel Wernand
Steef Peters

Intercomparison in the field between the new WISP-3 and other radiometers (TriOS Ramses, ASD FieldSpec, and TACCS)

Annelies Hommersom,[a,b] Susanne Kratzer,[a] Marnix Laanen,[b] Ilmar Ansko,[c] Martin Ligi,[c] Mariano Bresciani,[d] Claudia Giardino,[d] José M. Beltrán-Abaunza,[a] Gerald Moore,[e] Marcel Wernand,[f] and Steef Peters[b,g]

[a]Stockholm University, Department of Systems Ecology, 106 91 Stockholm, Sweden
hommersom@waterinsight.nl
[b]Water Insight, Postbus 435, 6700 AK, Wageningen, the Netherlands
[c]Tõravere Observatory, 61602, Tıravere, Tartumaa, Estonia
[d]National Research Council of Italy—Institute for Electromagnetic Sensing of the Environment (CNR-IREA), Via Bassini 13, 20133 Milan, Italy
[e]Bio-Optika, Crofters, Middle Dimson, Gunnislake, PL1 8 9NQ, United Kingdom
[f]Royal Netherlands Institute for Sea Research (NIOZ), Postbus 59, 1790, AB, Den Burg, Texel, the Netherlands
[g]Institute for Environmental Studies, de Boelelaan 1087, 1085 HA, Amsterdam, the Netherlands

Abstract. Optical close-range instruments can be applied to derive water quality parameters for monitoring purposes and for validation of optical satellite data. *In situ* radiometers are often difficult to deploy, especially from a small boat or a remote location. The water insight spectrometer (WISP-3) is a new hand-held radiometer for monitoring water quality, which automatically performs measurements with three radiometers (L_{sky}, L_u, E_d) and does not need to be connected with cables and electrical power during measurements. The instrument is described and its performance is assessed by an intercomparison to well-known radiometers, under real fieldwork conditions using a small boat and with sometimes windy and cloudy weather. Root mean squared percentage errors relative to those of the TriOS system were generally between 20% and 30% for remote sensing reflection, which was comparable to those of the other instruments included in this study. From this assessment, it can be stated that for the tested conditions, the WISP-3 can be used to obtain reflection spectra with accuracies in the same range as well-known instruments. When tuned with suitable regional algorithms, it can be used for quick scans for water quality monitoring of Chl, SPM, and aCDOM. [DOI: 10.1117/1.JRS.6.063615]

Keywords: WISP-3; radiometer; intercomparison; reflectance.

Paper 12122 received May 4, 2012; revised manuscript received Oct. 19, 2012; accepted for publication Nov. 27, 2012; published online Dec. 12, 2012.

1 Introduction

Monitoring water quality with optical close-range instruments and remote sensing has gained great attention since the establishment of the EU Water Framework Directive and with an increase in accuracy of the water quality parameters that can be derived from optical data.[1,2] Optical close-range instruments and satellites measure the light that is reflected by the water body. Algorithms are used to derive parameters such as chlorophyll-*a* (Chl-*a*) and suspended particulate matter (SPM) concentrations, the absorption by colored dissolved organic matter at 440 nm (aCDOM) and Secchi depth.[3] The advantage of optical measurements is that results can be available almost real-time. Satellite data can provide an overview over large areas with a single image. However, in small water bodies usually land influences the accuracy of the satellite

0091-3286/2012/$25.00 © 2012 SPIE

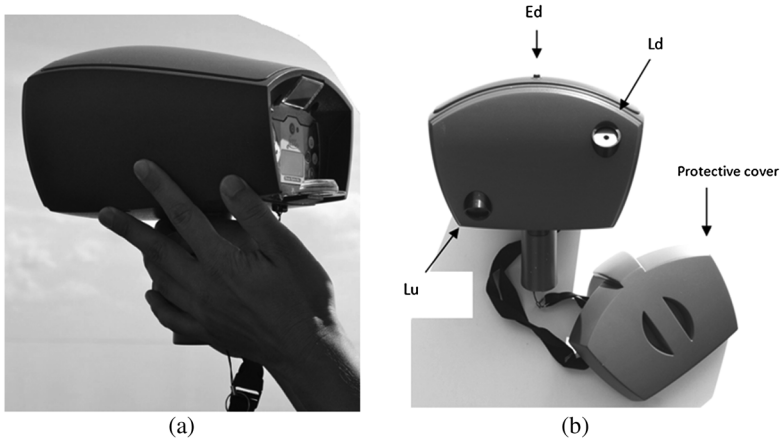

Fig. 1 WISP-3, handling (a) and an overview indicating the three radiometers (b).

data, whose spatial resolution may be still too coarse with respect to the size of the target. In these areas hand-held or autonomous close-range *in situ* optical instruments can be applied to derive water quality parameters.[4] The same *in situ* radiometers are also used for validation of reflectances derived with optical satellites.[5]

In situ radiometers can be difficult to deploy for routine monitoring of water quality parameters, especially from a small boat or on a remote location, for example, without electricity.[6] The water insight spectrometer (WISP-3) (Fig. 1) is a new hand-held radiometer for monitoring water quality. The WISP-3 is easy to handle and deploy, as it automatically performs measurements with three radiometers, it does not need to be connected to a laptop computer or electrical power point during measurements and can be taken to remote locations in a backpack. The instrument was designed for monitoring and research on water quality and can be used for optical satellite validation. For routine monitoring it derives concentrations of water quality parameters via standard algorithms, while remote sensing experts can use the spectral reflectance data and apply their own algorithms. The performance of the WISP-3 was assessed during inter-comparison field campaigns.

2 Materials and Methods

2.1 *WISP-3 Instrument*

The WISP-3 contains three Ocean Optics, Inc., JAZ radiometers, a portable computer, and a battery. The three radiometers are, via optical fibers, connected to, respectively a cosine corrector to measure the downwelling irradiance $[E_d(\lambda)]$, and two Gershun tubes to measure the downwelling radiance from the sky $[L_{\mathrm{sky}}(\lambda,\theta)]$ in which $\theta = 42$ deg from the zenith and the total upwelling radiance $[L_u(\lambda,\theta)]$ at 42 deg from the nadir ($\theta = 138$ deg). These three radiometers and the angles are chosen according to Mobley's[7] guidance on above-water radiometric measurements.

2.1.1 *Application*

Together, the three optical signals can be used to derive the reflectance of the water surface, which provides information on the contents of the water column. Based on dedicated algorithms, water quality parameters can be derived from reflectance spectra. Real-time concentrations of Chl-*a*, phycocyanin, and suspended matter are calculated using band ratio algorithms. The algorithms used for this can be adapted, depending on the water type where the measurements were taken. As a standard, the algorithms of Gons et al.[8] is used for Chl-*a*, the algorithm of Simis[9] is used for phycocyanin and an algorithm of Rijkeboer[10] is used for suspended matter. The results are shown on the display, providing monitoring staff with instant information. After uploading data to the web interface, more advanced algorithms, such as bio-optical models[11] can be applied to the data. The reflectance can be used for satellite validation, and one can also apply one's

own local algorithms on the data to derive information on water quality, such as Chl, SPM, and aCDOM.

2.1.2 *Characteristics*

The optical range of the WISP-3 is ~380 to 800 nm, with a band width (full width half max) of ~4.9 nm. The irradiance (spectral resolution of ~3.9 nm) is measured with an Ocean Optics CC3 cosine collector, the other two radiometers point at angles of 42 deg relative to the zenith and the nadir, to measure both radiance from the sky (band width of ~3.9 nm after boxcar averaging) and the water (band width of ~4.9 nm after boxcar averaging). Because it was noticed that the near infrared (NIR) wavelengths of the L_{sky} became less accurate under relatively dark conditions; in newer versions of the WISP-3 this channel is deployed with the same slit width as for L_u, so that the bandwidth is also ~4.9 nm. These spectrometers are fitted with optical fibers (diameter 400 μm) connecting to Ocean Optics Gershun tubes with 3 deg FOV apertures, respectively the CC3. The fibers are fixed in order to prevent moving. The WISP-3 weighs about 2.2 kg and is 24.7 cm long, 20.7 cm wide, and 15.5 cm high, 22 cm including the handle. Under standard settings, the WISP-3 takes five measurements for each radiometer in a total of 30 to 90 s (depending on the light intensity). It calculates the average L_{sky}, L_u and E_d and derives the average reflectance from these. It automatically corrects for dynamic dark readings, which are measured on a number of separate pixels that are not irradiated by external light during the measurements. Finally, the radiance L is derived from raw counts using Eq. (1), in which "cal" are the calibration values, t is the integration time of the measurement, A is the collection area (the surface of the optical fiber for the radiance measurements, the surface of the CC3 for the irradiance measurement), $d\lambda$ is the pixel width, and $\Omega = 2 * \pi * [1\text{-COS}(\mathrm{FOV}/2)]$, which is used to derive the radiance[12]

$$\mathrm{L}\ (\mathrm{mW\,m^{-2}\,nm^{-1}\,sr^{-1}}) = 0.01 * \left(\frac{\mathrm{counts} * \mathrm{cal}}{t}\right) \Big/ (A * d\lambda * \Omega). \tag{1}$$

The factor 0.01 converts $\mu\mathrm{W\,m^{-2}\,nm^{-1}\,sr^{-1}}$ to $\mathrm{mW\,m^{-2}\,nm^{-1}\,sr^{-1}}$. Irradiance $E\,(\mathrm{mW\,m^{-2}\,nm^{-1}})$ is calculated similarly, assuming $\Omega = 1$. All data is interpolated over 1 nm prior to further processing.

2.1.3 *Deployment*

WISP-3 measurements have to be taken at an azimuth angle of ~135 deg relative to the sun. In this way direct reflectance effects (e.g., sun glint) that occur at the surface are avoided as much as possible.[7] Angles <90 deg (toward the sun) and ~180 deg (opposite to the sun) should be avoided by the user. During measurements, the sun has to be >30 deg above the horizon because at lower sun inclination angles the light reflected at the surface will be measured primarily. The bulb on the WISP will assist in keeping the instrument horizontal so that the radiance is measured at an angle of 42 deg. As for other optical instruments, floating substances (plants, garbage, or foam), bottom visibility, self-shading of a boat or jetty, nearby trees or high buildings, and precipitation will lead to inaccurate measurements. Fully sunny or fully overcast skies will give the most accurate measurements; partial cloud cover can give a high fluctuation in the measured radiances. After a first evaluation of the results on screen, the data is saved on an SD card, which can be removed to transfer the data to a computer and web system interface. During our field campaigns, the WISP-3 was deployed according to these standards.

2.1.4 *Data processing*

The water leaving radiance $L_w(\lambda, \theta)$, measured at an angle of 42 deg relative to nadir ($\theta = 138$ deg), is calculated according to Eq. (2). For simplicity the + symbol for above water data has been left out in this work.

$$L_w(\lambda, \theta) = L_u(\lambda, \theta) - \rho_{\mathrm{sky}} * L_{\mathrm{sky}}(\lambda, \theta). \tag{2}$$

In Eq. (2), ρ_{sky} is the air–sea interface reflection coefficient, which is dependent on the wind speed (W) in m s^{-1}. Values for ρ_{sky} were taken from Mobley[7], except for the measurements carried out in the Wadden Sea, when wind speed was not measured, and ρ_{sky} was set to 0.028. In cases with wind <5 m s^{-1}, ρ_{sky} was also set to 0.028, which is standard for the WISP.

Subsequently, the uncorrected remote sensing reflectance $\mathrm{Rrs}(\lambda,\theta)$, at $\theta = 42$ deg relative to the zenith, is derived according to Eq. (3).

$$\mathrm{Rrs}(\lambda,\theta) = \frac{L_w(\lambda)}{E_d(\lambda)}. \tag{3}$$

For the assessments in this study, the $\mathrm{Rrs}(\lambda,\theta)$ spectra were subsequently corrected for a possible "white light" error ε, according to the method described by Ruddick et al.,[13,14] as shown in Eq. (4), in which $\alpha = 2.35$.

$$\varepsilon = \frac{\alpha * \mathrm{Rrs}(780) - \mathrm{Rrs}(720)}{\alpha - 1}. \tag{4}$$

The corrected remote sensing reflectance, $\mathrm{Rrs}_{\mathrm{corrected}}(\lambda,\theta)$, was derived by subtracting the error ε. For convenience, we will further refer to $\mathrm{Rrs}_{\mathrm{corrected}}(\lambda,\theta)$ with $\mathrm{Rrs}(\lambda,\theta)$.

2.1.5 *Accuracy*

The accuracy of the WISP-3 measurements is dependent on the sensitivity of the spectrometers, the calibration of the spectrometers, and a correct deployment (Fig. 1). The spectrometers, fibers, Gershun tubes and irradiance collector are produced by Ocean Optics Inc., USA. Ocean Optics estimates the signal-to-noise ratio of their single spectrometers as 250 : 1. The WISP is assembled and calibrated by Water Insight with a tungsten Ocean Optics second order calibration lamp, which is calibrated against a National Institute of Standards and Technology (NIST) traceable calibration lamp. Work on a calibration set-up for direct calibration with a NIST traceable lamp is in progress.

2.2 *Intercomparison*

2.2.1 *Aims and setup of the intercomparison*

Because the quality of the reflectance spectra determines the performance of the algorithms to derive water quality parameters, this intercomparison focuses on the quality of the obtained reflectance spectra.

After obtaining spectral reflectance of a water body, the retrieval of water quality parameters, such as Chl, SPM, or CDOM from reflectances is a next step. This can be done with various techniques, such as empirical algorithms based on band ratios, inverse modeling, or neural network approaches (Fig. 2). Differences in water types (e.g., clear waters in alpine regions, sediment rich waters in river discharges, and organic matter rich waters in Nordic regions) request regionally tuned algorithms. The development and tuning of regional algorithms is worth a study on its own.[15]

However, the quality of the reflectance spectra determines the accuracy of the algorithms to derive water quality parameters. Therefore, this intercomparison focuses mainly on the quality of the obtained reflectance spectra. Reflectance is also the parameter that is produced by all radiometers.

To show the possibilities to derive water quality parameters, also a short exercise is carried out on obtaining the correlation between water quality parameters (Chl, SPM, and aCDOM) and reflectance. In this study, we test band ratios proposed in the literature to derive water quality parameters from reflectance data. When specific inherent optical properties are available for an area, more dedicated algorithms, such as inverse models (Fig. 2) can be used and are expected to improve the retrieval of the different optical parameters.

The performance of the WISP-3 was assessed during three intercomparison field campaigns: in the Wadden Sea, the Netherlands, in Lake Peipsi, Estonia, and in Lake Vänern, Sweden. These water bodies have very different ranges of water constituents (Chl, SPM, and aCDOM).

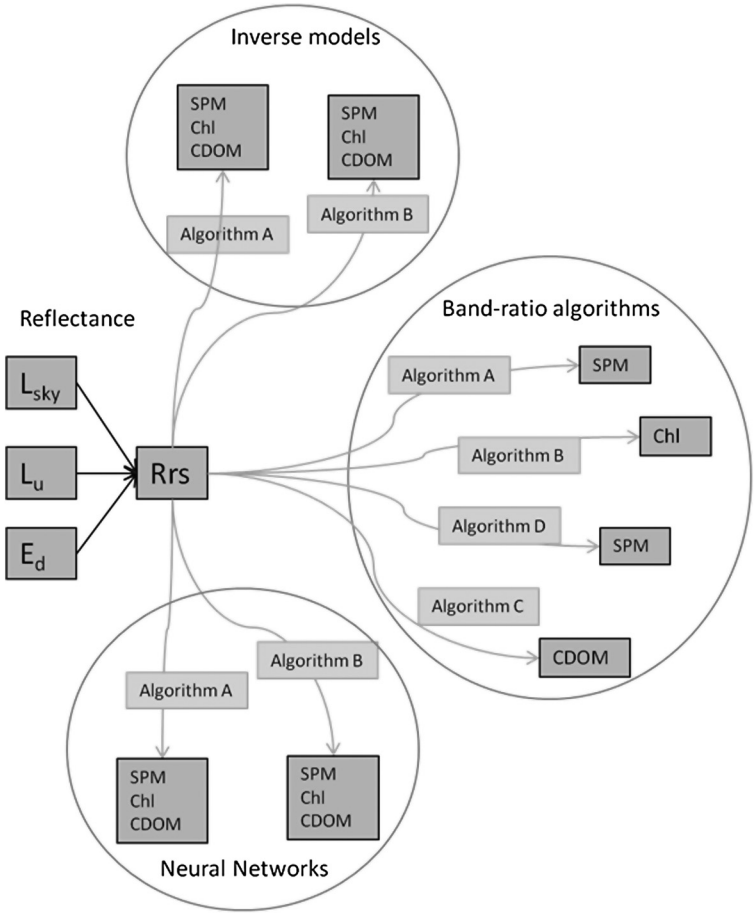

Fig. 2 Examples of how data from three radiometric measurements (L_{sky}, L_u, E_d) combined to Rrs, can be converted to water quality parameters.

Therefore, the magnitude and spectral shapes of the reflection spectra are very different and are expected to generate a valuable set of test cases. In the intercomparisons, the WISP-3 and radiometers widely used in validation of satellite data were deployed simultaneously.

The other radiometers included in this study are TriOS Ramses, ASD FieldSpec, and Tethered Attenuation Coefficient Chain Sensor (TACCS, Satlantic Inc., Canada) (Table 1); also, irradiance derived from a Microtops solar sensor is included. Due to dredging activities, the data of the SEA-PRISM radiometer at the at the Aeronet-Ocean Colour station[16] Pålgrunden could not be used.

First, on September 22, 2010, a WISP-3 instrument was tested at a jetty in the Wadden Sea, where a TriOS system (owned by the Netherlands Institute of Sea Research) is set up permanently. Second, on July 27, 2011, another WISP-3 instrument and another TriOS system (owned by Tartu Observatory) were deployed simultaneously in Lake Peipsi, Estonia. Finally, during a field campaign in Lake Vänern, Sweden, August 3-6, 2011, a third WISP-3 instrument, the TriOS system from Tartu Observatory, an ASD (owned by National Resource Council of Italy), a TACCS (owned by Stockholm University) and a Microtops solar sensor (owned by Water Insight) were deployed simultaneously. Intercomparison of these data sets was used for testing the WISP-3.

For most stations, measurements were obtained under changing cloud cover and with waves. Data obtained under such weather conditions cannot be used for intercalibrations, because the derived differences in the results are a combination of differences between the instruments and differences in the optical circumstances (i.e., changes in reflectance caused by changes in apparent optical properties induced by changes in cloud cover and wind-induced changes in water surface properties). However, the intention of this study is an intercomparison for the assessment of a new instrument. The results obtained at stations with less perfect conditions are

Table 1

Instrument	WISP-3	TriOS Ramses	ASD FieldSpec	ASD FieldSpec	TACCS
Deployment	Above water	Above water	Above water	Below water	Floating, below water
Radiometers	L_u, L_{sky}, E_d hyperspectral	L_u, L_{sky}, E_d hyperspectral	L_u, L_{sky}, E_d hyperspectral	E_d^{0-}, E_u^{0-}, L_u^0 hyperspectral	E_d (3 channel), $L_u^{0.5\ m-}$ (7 channel), chain of E_d^- (490 mm)-four depths
Method	Three radiometers	Three radiometers	One radiometer, E_d with RCR	One radiometer, E_d with RCR	Three radiometers, AC9 to derive spectral K_d^-
FOV (radiances)	3 deg	7 deg	6 deg	6 deg	10 deg
Angle relative to zenith and nadir	42 deg	Waddensea: 41 deg Peipsi and Vänern 40 deg	40 deg	0 deg	0 deg
Equations for Rrs	2–4	2–4	2–4	5,6	7–10
Extra corrections used for Table 2 and Fig. 5	Correction with hydrolight derived percentage difference between Rrs(λ,40) and Rrs(λ,0)				None

thought to be representative for the circumstances that will often be encountered in the field when the instrument is used operationally for monitoring. One can assume that the obtained errors will be smaller under stable weather conditions, while this assessment will give a fair estimate of the errors during rather common conditions during field work that may not be optimal regarding the weather and optical conditions.

2.2.2 *TriOS radiometers*

The TriOS radiometric measurement system consists of three TriOS-Ramses hyper spectral radiometers (350 to 950 nm). The radiometers can be deployed above or below water. In this study above-water systems were used: one irradiance sensor measuring E_d, and two radiance sensors with a FOV of 7 deg. TriOS was deployed at the front of the ship or jetty to avoid disturbance, and measurements were taken at an azimuth of 135 deg with respect to the sun. Rrs is calculated similar to the WISP-3, following Eqs. (2)–(4). The TriOS system used in the Wadden Sea had a set-up with radiance viewing angles of 41 deg relative to nadir for $L_u(\lambda,\theta)$ and zenith for $L_{sky}(\lambda,\theta)$, while the system used in Peipsi had radiance viewing angles of 40 deg relative to nadir and zenith. In Eqs. (2) and (3), θ differed therefore slightly. The TriOS system used in Vänern and Peipsi was calibrated against a NIST traceable 1000 W FEL lamp in Tartu Observatory. This particular system had performed very well as "TRIOS-E" in the "Assessment of *in situ* radiometric capabilities for coastal water remote sensing applications" (ARC-2010) intercalibration campaign at the Joint Reseach Center, Ispra, Italy,[17] showing absolute of relative percent differences (AD) in Rrs of 5.9%, 3.9%, and 7.2% at 443, 555, and 665 nm, respectively.[17] The TriOS system used in the Wadden Sea was calibrated at TRIOS GMBH. Except for the Wadden Sea station, five readings for each quantity were averaged before analysis.

2.2.3 *ASD FieldSpec radiometer*

The ASD FieldSpec is a hyper spectral instrument with a spectral range of 350 to 2500 nm. It can be deployed above and below water, and its FOV lenses can be changed. In this study radiances were measured subsequently with the same radiometer, deployed with a 6 deg FOV lens, while a remote cosine receptor (RCR) was mounted on the radiometer fiber to measure E_d. E_d, $L_{sky}(\lambda,\theta)$, and $L_u(\lambda,\theta)$ were measured above water with radiance viewing angles of 40 deg

relative to nadir $[L_u(\lambda,\theta)]$ and zenith $[L_{\text{sky}}(\lambda,\theta)]$. Additionally, measurements just below the water surface were made of the upwelling (E_u^{0-}) and downwelling (E_d^{0-}) irradiance and the upwelling radiance directly toward the zenith (L_d^{0-}). $\text{Rrs}(\lambda,\theta)$ can be calculated through Eqs. (2)–(4), but Rrs can also be calculated via Eqs. (5) or (6), using the in-water measurements, with $\theta = 0$ for L_u^{0-}.

$$\text{Rrs}(\lambda,\theta) = \frac{E_u^{0-}(\lambda)}{E_d^{0-}(\lambda) * Q * n_w^2}, \tag{5}$$

$$\text{Rrs}(\lambda,\theta) = \frac{L_u^{0-}(\lambda)}{E_d^{0-}(\lambda) * n_w^2}. \tag{6}$$

In Eqs. (5) and (6) the refractive index for water (n_w) is 1.34, and a factor $Q \sim \pi$ relates the upwelling irradiance to the upwelling radiance. For each quantity, the mean of five measurements was derived before analysis. The ASD spectroradiometers were calibrated using a NIST-traceable, 1000 W quartz-halogen lamp and a highly regulated power supply, producing a known irradiance, on a standardized Spectralon® diffuse reflectance panel. The instrument used in this work was calibrated in January 2011.

2.2.4 *TACCS radiometer*

The TACCS radiometer (Satlantic Inc., Canada) radiometer is deployed on a floating buoy. It has an in-air downward irradiance sensor (E_d) with three channels (443, 491, and 670 nm), a near surface (~50 cm depth) upwelling radiance sensor ($L_u^{0.5\text{ m}-}$) with seven channels at the ENVISAT-MERIS satellite bands (412, 443, 490, 510, 560, 620, and 670 nm); and a chain of E_d^- (490 nm) sensors at 2, 4, 6, and 8 m depth. All channels have a band width of 10 nm. The TACCS was deployed for 3 min taking samples at a rate of 0.5 Hz at 10 to 20 m distance from the ship to avoid ship shading. Simultaneously, depth profiles were taken with an ac9plus (WetLabs, www.wetlabs.com), measuring absorption (a) and beam attenuation (c) at 412, 440, 488, 510, 532, 555, 630, 676, and 715 nm. The instrument used in this work was calibrated in July 2010, and post deployment in January 2012. The instrument was not used before the post deployment calibration.

The TACCS and AC9 data were used together to derive the spectral reflectance.[3] The TACCS processing has been summarized in Zibordi et al.[17] and follows the MERIS optical measurement protocols.[18] A log-linear regression was applied to the four $E_d^-(490,z)$ measurements to derive $K_d(490)$, as the slope over the $\ln(E_d)$ versus depth graph. Next, $K_d(490)$ and AC9 data were combined to derive the spectral diffuse attenuation coefficient spectrum $K_d(\lambda)$.

After correcting the ac9 data for salinity and temperature,[19] the scattering (b) was derived as the difference between c and a. Both a and b were linearly interpolated to derive a and b at TACCS channels (412, 443, 490, 510, 560, 620, and 670 nm), due to the slightly different filters in the TACCS compared with the ac-9. Subsequently, spectral $K_d(\lambda)$ was derived from a and b via Kirk's Eq. (7).[20]

$$K_d(\lambda) = \mu_0^{-1}[a^2 + (g_1 * \mu_0 - g^2)a(\lambda) * b(\lambda)]^{0.5}. \tag{7}$$

In Eq. (7), the mean cosine of the refracted solar beam below the surface was assumed to be $\mu_0 = 0.86$ (which will provide the correct spectral shape, independent of solar angle θ), while the constants were $g_1 = 0.425$ and $g_2 = 0.19$.[20] The normalized K_d $[K_{d(\lambda)\text{norm}}]$ was calculated according to Eq. (8).

$$K_{d(\lambda)\text{norm}} = K_d(490) * K_{dac9}(490). \tag{8}$$

Then, $K_{d(\lambda)\text{norm}}$ was used to extrapolate the subsurface $L_u^{0.5\text{ m}-}(\lambda)$ to $L_u^{0-}(\lambda)$ by Eq. (9).

$$L_u^{0-}(\lambda) = \frac{L_u^{0.5\text{ m}-}(\lambda)}{e^{-0.5 * K_{d(\lambda)\text{norm}}}}. \tag{9}$$

Finally, $L_u(\lambda)$ (above water) was estimated by propagating $L_u^{0-}(\lambda)$ through the surface, using a surface term based on n_w.[17] Self-shading corrections were applied on $L_u(\lambda,0)$ according to

Mueller.[21] The self-shading correction requires: $a(\lambda)$, the diameter of the L_u sensor and the ratio of the diffuse to direct irradiance.[17] This ratio was derived from an irradiance model with input of the Microtops solar sensor and the three TACCS channels of E_d and the spectral shape from an irradiance model (see "Microtops" section for details). From the modelled spectral shape and the three E_d measurements, the downwelling irradiance $E_d(\lambda)$ at the other TACCS channels was derived.

Subsequently, Rrs was calculated according to Eq. (10).

$$\mathrm{Rrs}(\lambda,\theta) = \frac{L_u(\lambda)}{E_d(\lambda)}. \tag{10}$$

The TACCS was calibrated during the ARC-2010 campaign, where this particular system (TACCS-S) had shown AD values for Rrs of 4.5%, 6.1%, and 21.2% at 443, 555, and 665 nm, respectively.[17]

2.2.5 *Microtops solar sensor*

The Microtops solar sensor has to be pointed directly to the sun for a measurement. As precise pointing can be difficult, a series of measurements was taken at the stations where the TACCS was deployed. Measurement sets with high variance due to pointers errors were discarded and the remaining measurement sets were averaged. Because of practical reasons (having not enough manpower to deploy all instruments simultaneously), measurements at Station 1A were obtained 15 min before and 15 min after the time of the radiometric measurements and then averaged.

The Angström coefficient was derived by fitting a power function through the optical thickness at all wavelengths (440, 500, 675, 870, and 936 nm) and deriving the exponent. Water vapor, aerosol optical thickness and the Angström coefficient derived from the Microtops measurements were used as input for the irradiance model, together with local ozone concentration (http://jwocky.gsfc.nasa.gov/teacher/ozone_overhead_v8.html) and air pressure from the meteorological station at the nearby airport Såtanäs. An irradiance model, originally by Bird and Riorden[22] and improved by Thuillier et al.[23] was used to derive $E_d(\lambda)$ with a high resolution (details and updates can be found at http://rredc.nrel.gov/solar/models/spectral). The E_d spectral shape was also used for the TACCS data processing. For the Microtops, the producers' calibration coefficients were used.

2.2.6 *WISP-3 vicarious calibration*

After the campaign, the WISP-3 instrument used in Vänern appeared to have an invalid calibration. Therefore, a vicarious calibration relative to another WISP-3 instrument (owned by Water Insight) was made, based on a measurement under stable conditions in the harbor of Wageningen, the Netherlands. To do so, it was assumed that the spectral shapes obtained in the harbor should have been exactly the same. The calibration of the WISP-3 with the invalid calibration was adjusted so that the resulting spectral shapes were similar to those of the other WISP-3. The obtained vicarious calibration differed from the original calibration mostly in the blue wavelengths. The vicarious calibration was used to correct the measurements of the campaign in Vänern. For the WISP-3 instrument that was used as reference in the vicarious calibrations, the WISP-3 instrument used for the Wadden Sea and the WISP-3 instrument used in Lake Peipsi, the original calibrations by Water Insight made with a tungsten Ocean Optics calibration lamp were used.

2.2.7 *Analysis*

As $\mathrm{Rrs}(\lambda,\theta)$ is calculated with three radiometric spectra, instrument reliability can be best determined by comparing the three separate spectra, before analyzing the remote sensing reflectance. All radiometers and the solar sensor (TriOS, ASD, WISP-3, TACCS, and Microtops) provide E_d spectra which were compared. $L_{\mathrm{sky}}(\lambda,\theta)$ and $L_u(\lambda,\theta)$ spectra from TriOS, ASD, and WISP-3 were compared too. Finally, the end-product $\mathrm{Rrs}(\lambda,\theta)$ from TriOS, ASD, and WISP-3 and

$\mathrm{Rrs}(\lambda,\theta)$ from TACCS and ASD were compared. For two stations in Vänern, $\mathrm{Rrs}(\lambda,\theta)$ (from the above-water instruments) had to be compared with $\mathrm{Rrs}(\lambda,0)$ (from the below-water instruments). Instead of calculating normalized water-leaving radiances (e.g., Ref. 24), the relative difference between $\mathrm{Rrs}(\lambda,\theta)$ and $\mathrm{Rrs}(\lambda,0)$ for those stations where TACCS measurements were available was computed with the Hydrolight software. Hydrolight runs were made for Station 1A, which was on August 3, 2011, at 9.45 UTC, using Chl: 1.90 mg m^{-3}, SPM: 0.70 g m^{-3}, aCDOM: 1.00 m^{-1} (as measured *in situ*), including fluorescence and Raman scatter, assumed specific optical properties and phase function according to the Fournier-Forand phase function with $bb/b = 0.005$ for Chl and $bb/b = 0.010$ for SPM, a wind speed of 5 m s^{-1} and optically infinitely deep water. Output reflectance spectra were produced for 350 to 800 nm at 5 nm intervals and interpolated to 1 nm scale. The relative difference between the modelled $\mathrm{Rrs}(\lambda,\theta)$ and $\mathrm{Rrs}(\lambda,0)$ was found to be around $9\%(\lambda)$. This factor was used to convert $\mathrm{Rrs}(\lambda,\theta)$ from TriOS, ASD, and WISP-3 to $\mathrm{Rrs}(\lambda,0)$ for comparison with the TACCS and ASD for both stations 1A and 1B (for which the concentrations were very similar while there was just a 2-h difference in time).

Errors in the products $E_d(\lambda)$ and $\mathrm{Rrs}(\lambda)$ were quantified with the root mean square percentage error (RMSPE) [Eq. (11)], which gives a measure for the average percent error over the full spectrum.

$$\mathrm{RMSPE}(\%) = \sqrt{\frac{\Sigma \mathrm{PE}^2}{n}}. \tag{11}$$

In Eq. (11), n is the number of 1 nm wavelength increments. The multispectral character of TriOS, ASD, and WISP-3 allowed a comparison over the full spectral range. A wavelength range of 400 to 700, for which $n = 301$, is chosen, while in cases that the TACCS is included in the analysis $n = 7$, the number of TACCS bands. To derive the RMSPE, first the percentage error (PE) has to be calculated [Eq. (12)].

$$\mathrm{PE}(\lambda) = \frac{\frac{\mathrm{SX}(\lambda)-\mathrm{STriOS}(\lambda)}{\mathrm{STriOS}(\lambda)}}{100}. \tag{12}$$

In Eq. (12), the spectra (S) for the various instruments SX (with X is ASD, WISP-3, or TACCS) are compared to those of TriOS: first, because both the TriOS systems from Tartu Observatory and NIOZ have been tested and calibrated extensively, the former had performed very well in the ARC-2010 campaign,[17] and second, TriOS data was available for all stations. For comparison, also the average RMSPE between the five single TriOS measurements was calculated (TriOS within-station RMSPE).

Differences in the shape of the end-product Rrs are mainly due to differences in the measured products $L_{\mathrm{sky}}(\lambda,\theta)$, $L_u(\lambda,\theta)$, and $E_d(\lambda)$. However, $L_{\mathrm{sky}}(\lambda,\theta)$ and $L_u(\lambda,\theta)$ can only be compared quantitatively when the sensors are pointed in exactly the same direction because small differences in viewing angles might cause large differences in cases due to scattered clouds that are compensated for by calculating Rrs [Eq. (8)]. However, these single spectra might explain a large proportion of the errors in Rrs. $L_{\mathrm{sky}}(\lambda,\theta)$ and $L_u(\lambda,\theta)$ spectra were therefore plotted and qualitatively analyzed. When relevant, the standard deviation (St.dev.) between the five TriOS measurements is shown in the spectra as error bars.

After intercomparison of the reflectances, band ratios proposed in the literature are applied to the reflectance spectra and plotted versus *in situ* data of Chl, SPM, and aCDOM. As the TriOS and WISP-3 were deployed at a larger number of stations in Lake Vänern and Lake Peipsi, results of these two radiometers are used. From the Wadden Sea stations no *in situ* data was available for correlation. The band ratios tested are based on MERIS bands and specifically proposed for Vänern by Pierson and Strömbeck[25] [adjusted to MERIS bands by using Rrs (708) instead of Rrs(705)]. For Chl, the same band ratio was also proposed by Gons.[8]

$$\mathrm{Chl}:\ \mathrm{Rrs}(708)/\mathrm{Rrs}(665), \tag{13}$$

$$\mathrm{SPM}:\ \mathrm{Rrs}(708), \tag{14}$$

$$\mathrm{CDOM}:\ \mathrm{Rrs}(665)/\mathrm{Rrs}(490). \tag{15}$$

3 Results

3.1 *Wadden Sea*

On September 22, 2010, WISP-3, and TriOS measurements were taken at the NIOZ jetty in the Wadden Sea. Concentrations of the present substances were not measured. It is known, however, that the reflectance of the Wadden Sea is mostly caused by SPM.[26] Wind speed has not been measured directly, but the wave height was estimated to be between 10 and 20 cm. The strong reflection by SPM became visible in the magnitude of the Rrs spectrum with a maximum around 0.015 sr^{-1} [Fig. 3(d)]. In this campaign, measurements were taken at exactly the same moment with the sensors looking in the same direction, so also L_u and L_{sky} spectra were compared.

The measured L_{sky} spectra agreed well between TriOS and WISP-3, with a RMSPE of 10% (Fig. 3). For L_u the RMSPE was somewhat higher, 20% on average. For both radiance measurements the spectral shapes generally correspond well, although L_{sky} shows some noise between 380 and 400 nm, while WISP-3 and TriOS do not have exactly the same shape for L_u in the 380 to 500 nm spectral region. The higher WISP-3 values in L_u near 500 nm seem to be caused by a higher influence of directly reflected sunlight because this effect does not appear in the Rrs spectrum. The shape of the E_d spectra also agreed well, but with a relatively large RMSPE of 21%. The differences in E_d can probably be explained by the fact that the TriOS system was set up on a tall pole at the NIOZ jetty, to avoid shading by other equipment and a small white shed, while the WISP-3 was deployed manually on "jetty level.". The lower E_d values may therefore have been caused by the blocking of diffuse sunlight by the small shed. When Rrs was corrected for the percentage difference in E_d, RMSPE values for Rrs decreased subsequently from 76% to 47%.

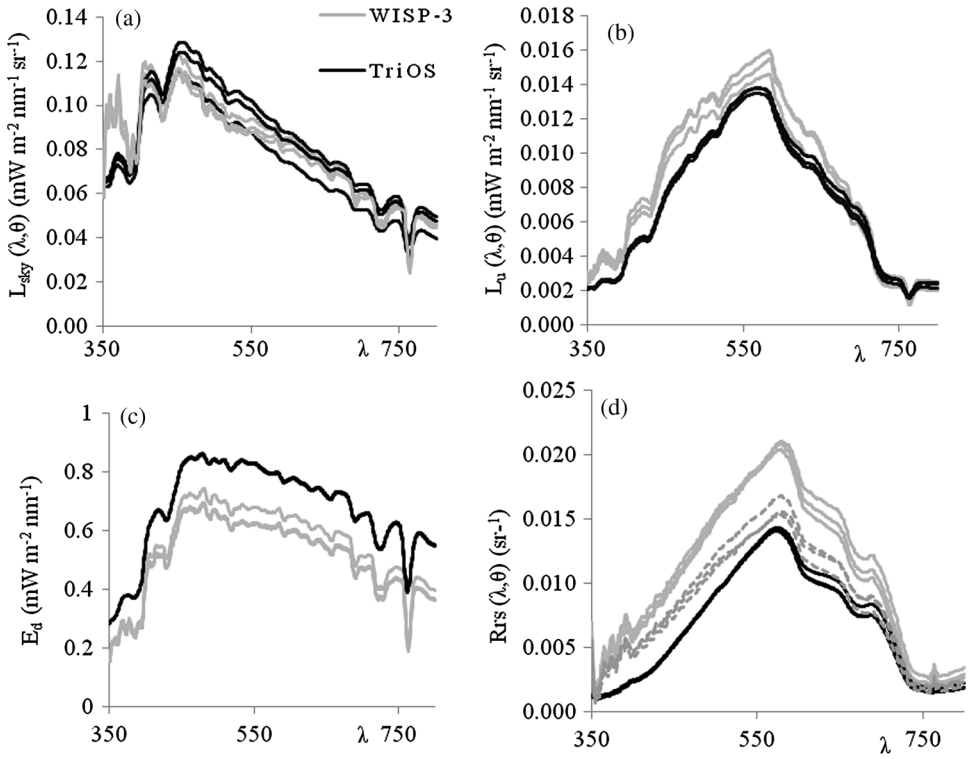

Fig. 3 Results of three single measurements of TriOS and WISP-3 at the NIOZ Jetty in the Wadden Sea. (a) $L_{sky}(\lambda,\theta)$, RMSPE = 12%, 7%, 12% for the three WISP-3 measurements versus TriOS. (b): $L_u(\lambda,\theta)$, RMSPE = 23%, 25%, 13% for the three WISP-3 measurements versus TriOS. (c) $E_d(\lambda)$ RMSPE = 23, 17%, 23% for the three WISP-3 measurements versus TriOS. (d) Rrs(λ,θ), RMSPE = 79%, 75%, 73% for the three WISP-3 measurements versus TriOS, and 48%, 50%, 43% for the corrected WISP-3 measurements (dashed) versus TriOS.

3.2 *Lake Peipsi*

On July 27, 2011, WISP-3 and TriOS measurements were taken on Lake Peipsi, Estonia. During those days, wind speeds were 1 to 2 $m\,s^{-1}$ and the sky was mostly covered by cirrus clouds, with up to 15% cumulus coverage at the horizon. There was a high and relatively constant influence of aCDOM (2.58 to 2.95 m^{-1}) at all sampling stations in Lake Peipsi, a somewhat smaller and also relatively constant influence of SPM (9.00 to 9.76 $g\,m^{-3}$), while most of the variability in Rrs was caused by Chl: 22.7 to 46.73 $mg\,m^{-3}$. The influence of the high Chl concentrations is visible in the Rrs spectra by the pronounced absorption trough near 675 nm, next to the relative high Rrs values due to SPM scatter around 700 nm. Due to the high aCDOM the spectra are generally dark, i.e., with low reflectance values, compared to those of the Wadden Sea, especially in the blue region (350 to 500 nm), while Chl absorption is clearly visible around 672 nm [Fig. 4(g) and 4(h)].

Because it would be space-consuming to present all data from Peipsi, the data from the station with the highest RMSPE in Rrs (Station 1) and the lowest RMSPE (Station 4) are shown (Fig. 4). L_u measurements in Peipsi agreed relatively well between WISP-3 and TriOS measurements (RMSPE 9% to 25% for all five stations). In L_{sky} the problems related to partial cloud cover are more pronounced: for Station 4 the agreement is very good (RMSPE = 3% and for almost the whole spectrum the WISP-3 values are within the standard deviation of the TriOS measurements), but for Station 1 RMSPE = 35%. RMSPE at the other three stations ranged from 15% to 21%. For E_d RMSPE ranged 17% to 40% over the five stations. Probably, the WISP-3 measurement at Station 1 (RMSPE = 40%) was carried out when the sun had just moved behind a cloud. When L_u has been measured at a spot that received less sunlight than may be expected from the L_{sky} measurement, Rrs shows negative values in the blue wavelengths, as can be seen in Rrs of Station 1. The relatively low E_d compared to TriOS causes the overall relatively high Rrs, while the somewhat higher L_{sky} causes the steep spectral shape in the 380 to 480 region. The WISP-3 has the same effect at Station 4, which could be the same effect or could indicate a calibration error for either the L_u or the L_{sky} radiometer.

3.3 *Lake Vänern*

On August 3, 2011, the WISP-3, TriOS, ASD FieldSpec, TACCS, and the Microtops solar sensor were deployed simultaneously in the open part of the western basin of Vänern. The weather conditions were relatively good: blue sky with thin cirrus clouds and almost no wind (0 to 1.4 $m\,s^{-1}$). Data from the two stations on this day (stations 1A and 1B, 58.70618N, 12.84023E at 09.45 UTC, respectively 58.6933N, 12.7354E at 10.30 UTC) were the most important intercomparison stations for this work, because all instruments were available and there were almost no disturbing waves. The optical properties of the water at stations 1A and 1B were dominated by high concentrations of aCDOM (1.06 m^{-1} at both stations) and by Chl (1.96, respectively 1.80 $mg\,m^{-3}$). SPM concentrations were relatively low (0.63, respectively 0.52 $g\,m^{-3}$). Subsequently, the recorded Rrs was low (with a maximum around 0.0018 sr^{-1}, i.e., only about a tenth of the reflection in the Wadden Sea).

At stations 1A and 1B in Vänern, the recorded L_{sky} spectra (Fig. 5) were very similar for the TriOS, WISP-3 and ASD. Also the E_d measurements of TriOS and WISP-3 were similar, with a RMSPE of 8% (Table 2), and closely related to the E_d spectra derived with Microtops and HYDROLIGHT. However, E_d values from Microtops show water vapor dips around 690 nm that are too strongly pronounced. This is due to overestimated water vapour absorption values in the irradiance model. The ASD E_d spectra were lower than the reference [Fig. 5(e) and 5(f), RMSPE = 28%]. This is presumably caused by boat shadowing, when the measurements were taken manually just above the water surface right by the side of the boat. Although the recommended number of 25 measurements[27] was not reached (at Station 1A, 17 measurements were taken, at Station 1B 7) the derived E_d spectra were very similar to those of TriOS [Fig. 5(e) and 5(f)] and therefore the derived values were assumed to be suitable for the TACCS processing. E_d spectra of the TACCS are expected to be influenced by geometric effects (tilt and roll).

The water measurements from the above-water instruments are influenced by direct sky reflection. This effect is supposed to be taken away through ρ_{sky} in Eq. (2), which worked

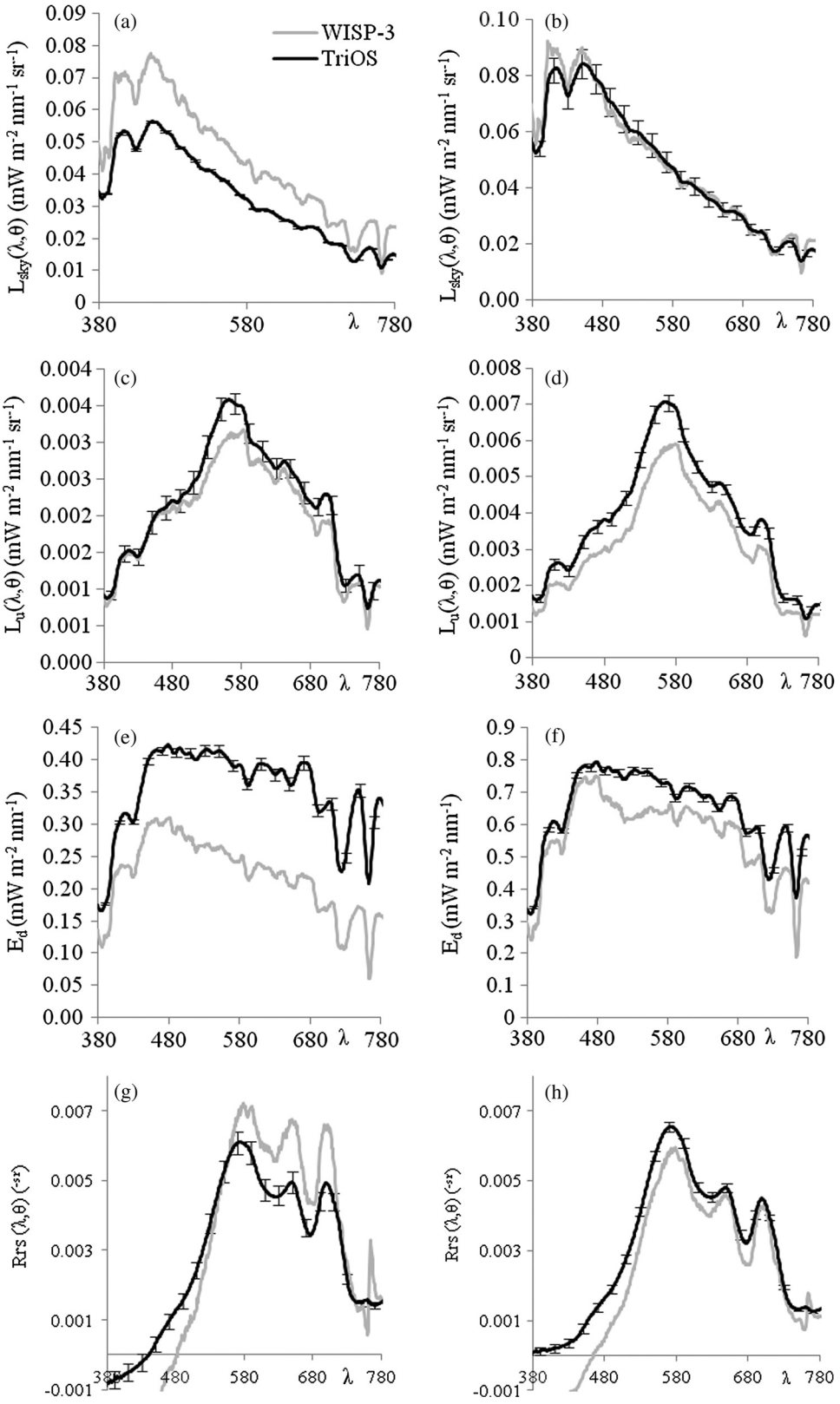

Fig. 4 Results for TriOS and WISP-3 at two stations in Lake Peipsi. Left panels for station 1, right panels for station 4. RMSPE values for TriOS-within station and WISP-3 versus TriOS were respectively: (a) $L_{sky}(\lambda,\theta)$, RMSPE = 5%, 35%. (b) $L_{sky}(\lambda,\theta)$, RMSPE = 3, 22%. (c) $L_u(\lambda,\theta)$, RMSPE = 2%, 9%. (d) $L_u(\lambda,\theta)$, RMSPE = 5%, 26%. (e) $E_d(\lambda)$, RMSPE = 2%, 39%. (f) $E_d(\lambda)$, RMSPE = 1%, 18%. (g) Rrs(λ,θ), RMSPE = 6%, 32% (derived 483 nm > because of negative values in the blue). (h) Rrs(λ,θ), RMSPE = 3%, 22% (derived 465 nm > because of negative values in the blue).

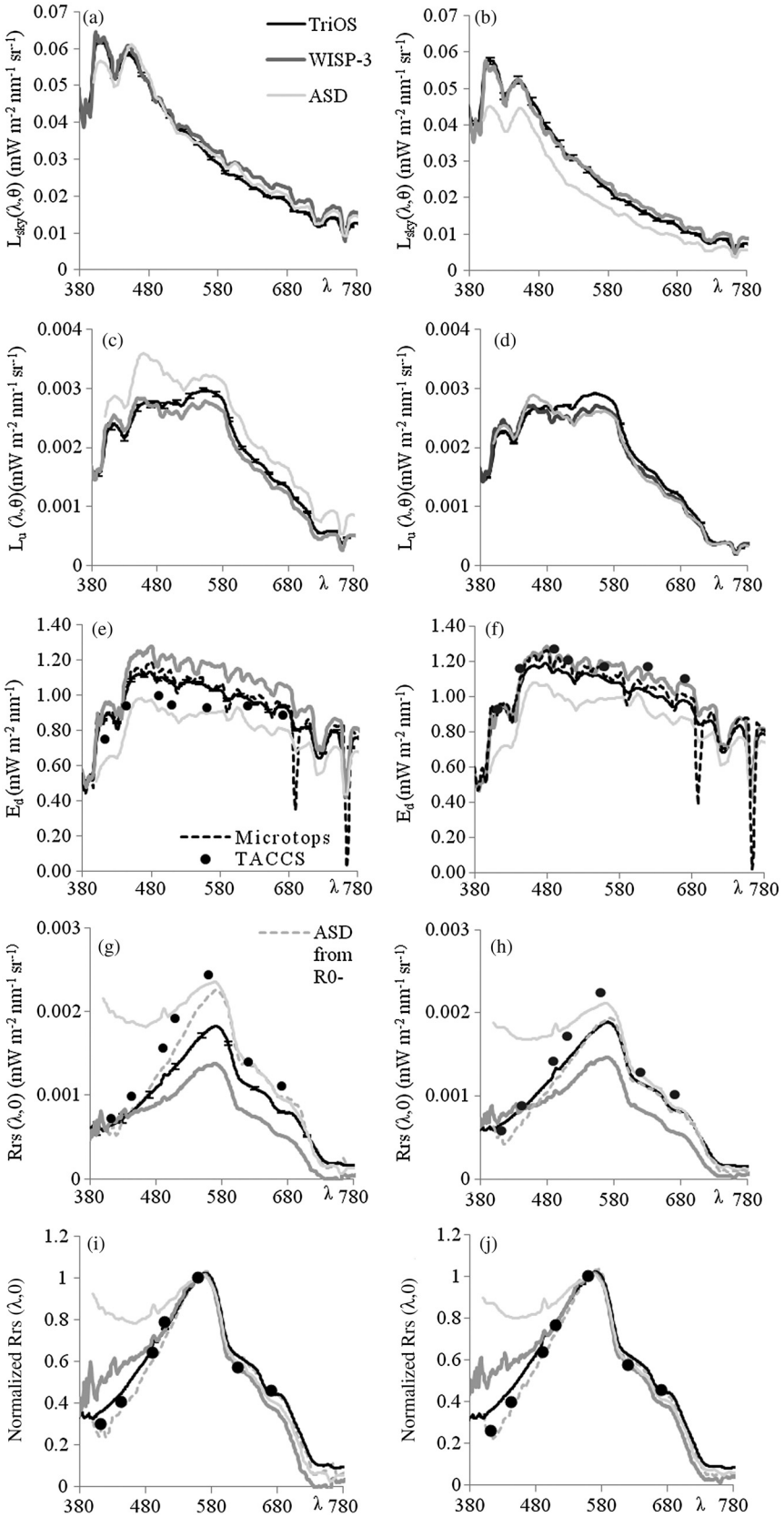

Fig. 5 Results of TriOS, WISP-3, ASD, Microtops, TACCS, and ASD below-water measurement via Eq. (4), at a station 1A (left panels) and 1B (right panels) in Vänern. (a) and (b) $L_{sky}(\lambda,\theta)$, (c) and (d) $L_u(\lambda,\theta)$. (e) and (f) $E_d(\lambda)$, (g) and (h) $\mathrm{Rrs}(\lambda,0)$. RMSPE values are presented in Table 2, (i) and (j) $\mathrm{Rrs}(\lambda,0)$ spectra normalized at 560 nm.

Table 2 Root mean squared percentage errors for stations 1A and 1B. Each instrument is compared to the TriOS system from Tartu Observatory.

RMSPE (%) ($n = 7$)	Station 1A		Station 1B	
	E_d	Rrs	E_d	Rrs
TriOS (within station)	0	4	0	1
WISP	8	24	2	22
ASD (above water)	28	102	25	78
ASD via Eq. (4)	—	17	—	13
TACCS	8	32	25	16

well for TriOS. But for the ASD, and to a minor extent the WISP-3, there was still an influence visible in the blue wavelengths (<480 nm) of the Rrs spectra [Fig. 5(g) and 5(h)]. However, the underwater measurements of the ASD were not affected by sun glint and showed much lower RMSPE values of 17% and 13%, respectively [Fig. 5(g) and 5(h), Table 2].

On August 4, 2011, WISP-3, TriOS, ASD, and Microtops measurements were taken at 10 stations (E1 to E10) in the southern part of the eastern basin of Vänern, with variable concentrations of water constituents. The weather conditions varied from scattered clouds to almost full overcast, with wind speed ranging from 1.9 to 5.5 $\mathrm{m\,s^{-1}}$. At some of the stations, the optical measurements were difficult to perform from the small boat due to relatively large wave action. Small boats were required, though as the water was rather shallow. This data shows the reliability of the sensors under less favorable conditions (Fig. 6). The optical water constituents were also much more variable than in the open lake with Chl: 1.02 to 11.49 $\mathrm{mg\,m^{-3}}$, SPM: 0.58 to 4.53 $\mathrm{g\,m^{-3}}$, aCDOM: 1.15 to 4.68 $\mathrm{m^{-1}}$.

At stations E1 to E10 the general findings from stations 1A and 1B continued: L_{sky} was generally similar in spectral shape for TriOS, ASD, and WISP-3, although the intensity varied because of cloud scatter. L_u measured with the ASD and, to a minor extent, the WISP-3, contained too much direct sky reflectance at stations with stronger wave action. E_d was similar in shape but lower for the ASD. Therefore, in Fig. 6 only Rrs spectra are presented for these stations. For eight of these 10 stations the below-water measurements from ASD [via Eq. (4)] showed Rrs spectra that were very similar in shape to those of TriOS; however, those are not presented here because of the difference in viewing geometry.

For the Stations E1 to E10, with varying wave conditions, TriOS gave the most stable Rrs results, although negative values in the blue occurred at two stations. For these stations the RMSPE could not be calculated. The WISP-3 performances were more stable than the ASD above-water measurements, although Rrs was too high in the blue and somewhat too low in the green. However, for measurements taken from a small boat, with relatively high waves and scattered clouds, a high RMSPE (between 20% and 30%, except of one positive outlier of 17% and one negative outlier of 38%) seems reasonable. A considerable part of the error was due to waves, and changing conditions can be derived from the fact that TriOS measurements at certain stations had RMSPE values ranging 4% and 19%, with an outlier of 26%.

For the ASD the effect in the blue wavelengths is most likely caused by a wrong viewing angle relative to the nadir, because the ASD has to be pointed manually towards the correct angles. Adapting ρ_{sky} could probably improve the results. However, it might be difficult to determine what the final result of an iteration would be. For the WISP-3, the smaller FOV could be a reason as to why the instrument is more vulnerable for this type of error. However, the results from the Wadden Sea and Lake Peipsi do not show similar effects, while the effect can be seen to a lesser extent at almost all stations in Vänern. Therefore, it is possible that the vicarious calibration of the instrument used in this lake was less accurate at those wavelengths. At two stations with relatively large waves, the TriOS measurements also failed by producing a Rrs spectrum with negative values in the blue.

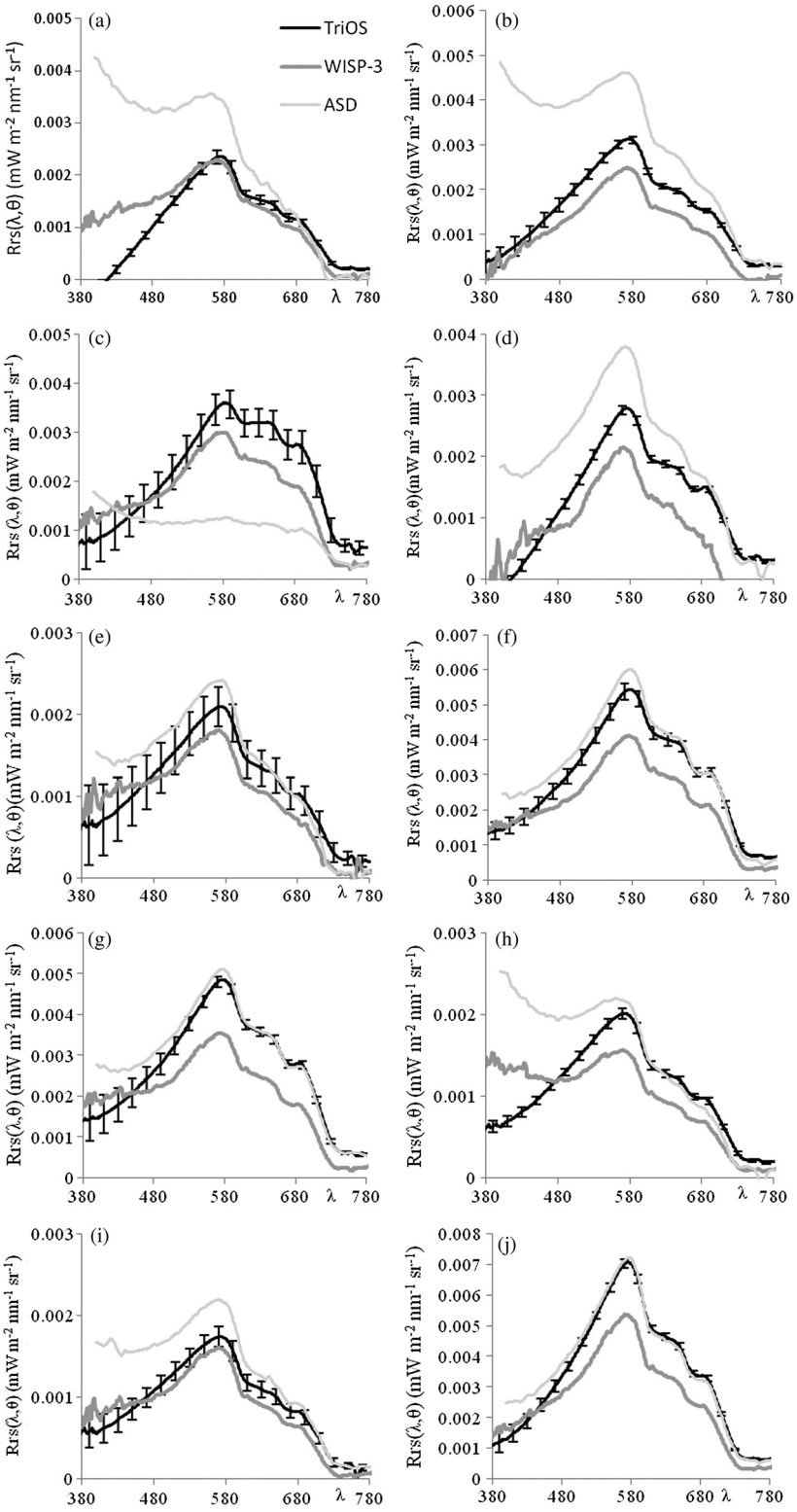

Fig. 6 Remote sensing reflectance Rrs of TriOS, WISP-3, and ASD at various (coastal) locations in Vänern. RMSPE values for TriOS-within station, WISP versus TriOS and ASD versus TriOS were, respectively: (a) Station E1, RMSPE not available. High wave action. (b) Station E2, RMSPE = 8%, 27%, 220%. (c) Station E3, RMSPE = 17%, 25%, 69%. (d) Station E4, RMSPE not available. High wave action. (e) Station E5, RMSPE = 19%, 22%, 40%. (f) Station E6, RMSPE = 65%, 23%, 21%. (g) Station E7, RMSPE = 9%, 26%, 25%.(h) Station E8, RMSPE = 4, 38, 91%. High wave action. (i) Station E9, RMSPE = 11%, 17%, 65%. High wave action. (j) Station E10, RMSPE = 5%, 23%, 23%.

Finally, three stations (D1 to D3) in the shallow basin Dättern on the southern side of Vänern were visited on August 6, 2011. Here, the wind had increased to 4 to 10 $m\,s^{-1}$. The optical water constituents at these stations were: Chl: 15.68 to 36.41 $mg\,m^{-3}$, SPM: 16.28 to 31.40 $g\,m^{-3}$, aCDOM: 3.20 to 9.54 m^{-1}.

During the measurements in Dättern, the weather conditions worsened, while the wind force increased wave height and therefore the resuspension of sediments. Therefore, there are large differences in all three radiometric measurements, as well as in the derived remote sensing reflection. Despite these circumstances, the spectral shape of L_u of all three recorded spectra by TriOS and WISP-3 were very similar [Fig. 7(b)]. For the separate measurements of L_{sky}, L_u and E_d, the WISP-3 had RMSPE values that were similar to those of TriOS-within station (Fig. 7).

After applying the white light correction according to Ruddick et al.[14], Eq. (4), the Rrs-spectra of both TriOS and WISP-3 turned negative for the stations in Dättern. Doron et al.[28] showed that the NIR-based correction does not have the same value for α at locations with high turbidity (such as SPM concentrations >30 $mg\,m^{-3}$) and/or highly absorbing SPM. The spectral effects of an inappropriate value for α in their simulated spectra are largest in the blue and NIR. From *in situ* samples it is known that the SPM in Dättern has indeed an extremely high weight-specific absorption coefficient: $a{*}_{SPM}(440)$ ranged between 0.113 $m^2\,g^{-1}$ at station D1 and 0.099 $m^2\,g^{-1}$ at station D3, while the average of 0.067 $m^2\,g^{-1}$ of the Baltic Sea found by Babin et al[29] was also high compared to that in other European seas.[29] SPM concentrations were also rather high: 16 $mg\,m^{-3}$ at D1 and 30 to 31 $mg\,m^{-3}$ at stations D2 and D3. Therefore, we tried several values for α in Eq. (4), so that the reflectances were just above zero at 380 nm for both instruments (applying one α value per station for both instruments). Finally, α was adjusted to 1.6 at station D1 and 2.2 at stations D2 and D3. The WISP-3 RMSPE values around 39% (calculated for D2) seemed to be mainly due to difference in sky measurements: at station D1 the E_d measurements were the main cause of the differences, although for <450 nm also the L_u spectra varied, and at stations D2 and D3 the L_{sky} measurements differed most from TriOS. Therefore, the discrepancies in the Rrs spectra can, via the E_d and L_{sky} measurements, be related to the changing cloud cover during the measurements.

3.4 *Correlations of Band Ratios with In Situ Concentrations*

Band ratios from TriOS, WISP-3, and ASD measurements were plotted versus *in situ* derived concentration values [Fig. 8(a)–8(c)]. The chlorophyll data showed the most scatter [Fig. 8(a)]. The influence of Chl on the reflectance spectrum is probably most influenced by that of the other optical substances. The Rrs(665) band proposed for the retrieval of Chl is to a certain extent influenced by aCDOM absorption, while Rrs(708) is strongly influenced by SPM scattering [Fig. 8(b)]. SPM is the best retrieved water quality parameter [Fig. 8(b)]. With a very simple one-band algorithm and a linear function it can be retrieved from the measured reflectance. For aCDOM [Fig. 8(c)], the data from the stations in Lake Peipsi are not included in the scatterplot because the CDOM algorithm did probably not suit for this water type. The aCDOM values were all between 2.58 and 2.95 m^{-1}, in Lake Peipsi, while the band ratio seemed to be influenced by another substance, leading to a bad correlation (for TriOS, but worse for the WISP-3, no data available for the ASD). The outlier in the scatterplot (aCDOM = 4.68 m^{-1}), was measured at the station that was located exactly in the mouth of the River Lidan. Therefore, the optical properties found at this station were probably rather different from those in the open lake Vänern, which may explain why the correlation is somewhat different for this station. Generally, however, band ratios from the radiometers resulted in correlations with high correlation-coefficients for all three water quality parameters, with $R^2 = 0.80$, 0.86, and 0.86 for TriOS, WISP-3, respectively ASD for the log-plot between $\mathrm{Rrs}(705)/\mathrm{Rrs}(665)$ and Chl; $R^2 = 0.98$, 0.88, 0.93, respectively for the linear plot between Rrs(750) and SPM; and $R^2 = 0.91$, 0.83 and 0.62 for TriOS, WISP-3, respectively ASD for the log-plot between $\mathrm{Rrs}(665)/\mathrm{Rrs}(490)$ and aCDOM. Based on these correlations, algorithms can be constructed to derive the water quality parameters accurately from obtained reflectances. The band ratio algorithms can be programmed into the WISP-3 so that concentrations of water quality parameters will be shown directly on screen after the measurement.

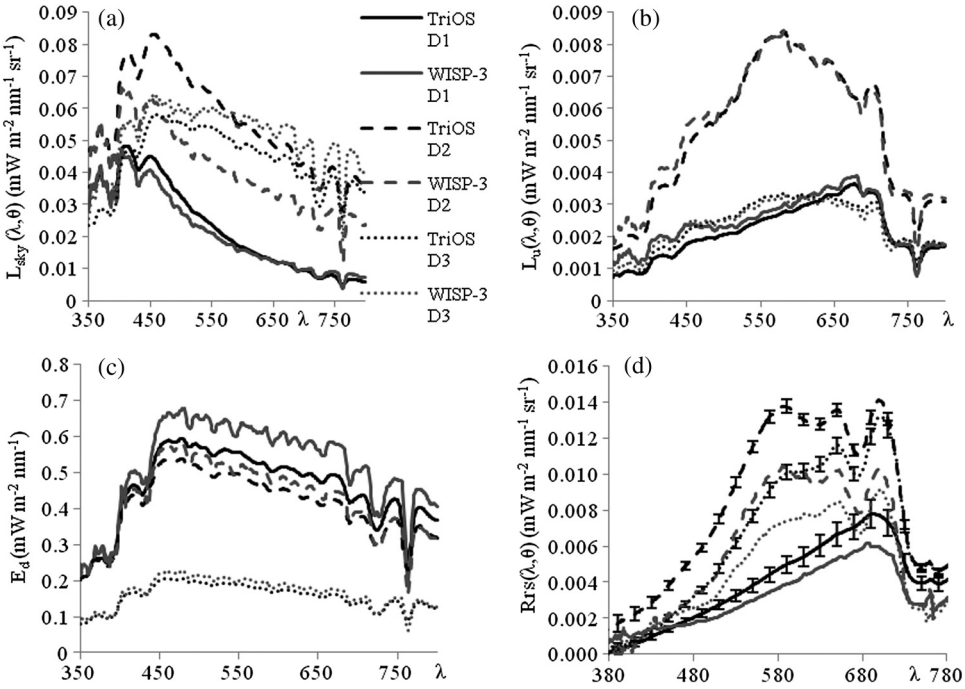

Fig. 7 TriOS and WISP-3 measurements at stations stations D1, D2, and D3 in the turbid bay Dättern on the southern side of Vänern. Station D1 was partially cloudy, and at D2 and D3 the sky was fully covered. At D3 the wind induced relatively large waves. RMSPE for D1, D2, and D3 were, respectively: (a) $L_{sky}(\lambda,\theta)$, RMSPE = 19, 5, 8% (TriOS within-station); 9, 30, 18% (WISP-3). (b) $L_u(\lambda,\theta)$, RMSPE = 7%, 20%, 12% (TriOS within-station); 20%, 7%, 7% (WISP-3). (c) $E_d(\lambda)$, RMSPE = 19%, 4%, 5% (TriOS within-station); 15%, 6%, 9% (WISP-3). (d) Rrs(λ,θ), RMSPE = 10%, 5%, 7% (TriOS within-station); 35%, 39%, 26% (WISP-3).

4 Discussion

In this assessment the performance of the new WISP-3 radiometer was compared to well known radiometers. The intercomparisons did not take place under perfect (weather) conditions. Therefore, the results showed errors that were larger than necessary, and hence the results are thought to be representative for general, nonoptimal fieldwork conditions, while the derived RMSPE values can be assumed to be smaller under stable weather conditions. However, it would be desirable to participate in a dedicated intercalibration exercise with the WISP-3 under stable measurement and weather conditions, such as the ARC-2010 campaign,[17] which took place when only an early prototype WISP-3 was available.

WISP-3 RMSPE values for Rrs relative to TriOS measurements were generally between 20% and 30%. Higher values were only found under very rough conditions (partly cloudy, measured from a small boat under wavy conditions, at not exactly the same time) and in high-reflecting waters in the Wadden Sea.

At the most stable stations, 1A and 1B, RMSPE values were 24% and 22%, respectively, whereas the reference, TriOS, showed 3% and 1% difference, respectively, between measurements. Therefore, at these two stations we assume an error of 3% and 1%, respectively due to wave action. Assuming also a calibration difference of 3% because of using different calibration sources and because of the vicarious calibration of the WISP-3, this leaves a remainder of 18% error for the WISP-3 for stations 1A and 1B. Part of the higher error of the WISP-3 will be caused by measuring at not exactly the same moment and by pointing at not exactly at the same water area and sky position. The 8% RMSPE for E_d indicates the latter for station 1A, as at station 1B the RMSPE for E_d was only 2%. The difference in E_d has an influence of ~7% on Rrs at station 1A. However, the largest effect is caused by differences in L_u. When the L_u measured with the WISP-3 is substituted with the L_u measured with TriOS, the RMPE is reduced to 6%, respectively 7% at once. In the ARC-2010 campaign this particular TriOS system itself had a spectral averaged AD value of ~6% with regards to the reference.[17]

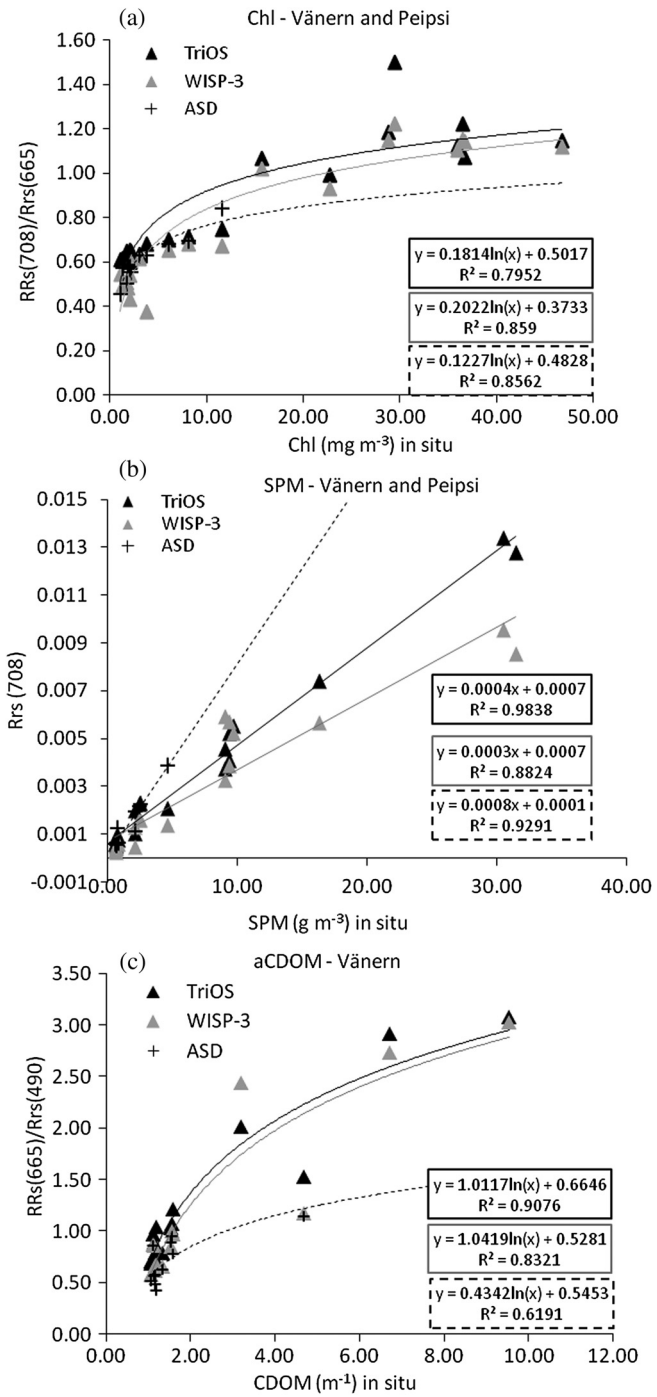

Fig. 8 Band ratios from Ref. (26) derived from reflectance spectra of TriOS (black triangles), WISP-3 (gray triangles) and ASD (plus-signs) at the stations in Vänern and Peipsi, for aCDOM only for Vänern versus *in situ* measured concentrations. Note that ASD measurements were only taken in the main basin of Lake Vänern, not in the basin Dättern and Lake Peipsi. Trend lines and correlation coefficients are shown next to the scatterplots (TriOS black, WISP-3 gray, ADS dashed).

The error in L_u recorded by the WISP-3 is mainly caused by a lower reflectance in the yellow-green (480 to 680 nm) region compared to the TriOS system. At the same time, the TACCS and ASD underwater measurement overestimated the reflectance in this spectral range. However, the sensitivity of the WISP-3 in the yellow-green spectral region in dark waters should receive attention in future intercomparisons and intercalibrations. After normalization the spectral

shapes are very similar for wavelengths >480 nm. For the WISP-3 the vicarious calibration is expected to have played a role at smaller wavelengths, as similar differences in the blue do not occur for the measurements in the Wadden Sea and Lake Peipsi.

In the ARC-2010 campaign the particulate TACCS used in this study has been proven to have a spectral averaged AD value of 5.3% over the blue-green spectral region, and 21.2% in the red, which was in the same order of magnitude as the other instruments considered.[17] Note that the higher error in the red may be due to the low number of red photons at 50 cm depth measured by the L_u sensor, leading to a higher error in the measurement. At stations 1A and 1B the RMSPE values of the WISP-3 measurements (24% and 22%, respectively) were comparable with those of the TACCS data (RMSPE values of 32% and 16%, respectively), much lower than those of the ASD above-water measurements (RMSPE values of 102% and 78%, respectively) and somewhat higher than those of the ASD below water measurements (RMSPE values of 17% and 13%, respectively). Therefore, it can be stated that the errors within the measurements of the WISP-3 are comparable to those of other radiometers used for validation.

In many cases, the three separate radiometric measurements (L_{sky}, L_u, E_d) showed much lower RMSPE values than the derived Rrs. L_u was the least accurate of the three separate measurements, for the above-water measurements, which can be explained by the unknown proportion of direct sky reflection that is included in this measurement. For the TACCS, L_u is the most reliable measurement.[17] In above-water measurements, the blue side of the spectrum is most vulnerable for this type of error.[7]

So, by combining the TACCS L_u measurements with the Microtops E_d measurements, the error can be reduced. Under partially cloudy conditions, logically L_{sky} and E_d were variable, which made it difficult to determine which differences in Rrs spectra were due to real differences in conditions and which portion was due to differences in instrument accuracies.

For the above-water instruments, TriOS gave the most stable measurements in this assessment: there were only invalid TriOS spectra at four stations, while none of the TriOS spectra showed strong influence of direct sky light. The ASD above-water reflectances were least stable, mainly due to errors in the L_u spectrum. In-water measurements of the ASD did not suffer from the sun glint effect and showed lower RMSPE values. ASD below-water measurements were generally reliable, which is also expected from the TACCS. However, above-water measurements are much easier to perform than in-water measurements, which is the advantage of the TriOS, WISP-3, and ASD. Also, the processing of the TACCS data is extremely complex (including a solar model to derive a spectral E_d). From the TACCS only data from two stations was available, due to limiting space on the small boat and the shallowness of the water. The TACCS can only be deployed in water deeper than 10 m because of the length of the K_d chain.

One advantage of the WISP-3 is its higher spectral resolution (~4.9 nm) relative to the TriOS (~10 nm). The higher spectral resolution is especially pronounced in the E_d spectrum, which has a spectral resolution of ~3.9 nm: much more detailed features are visible [e.g., the ozone absorption dips, Fig. 7(c)]. This higher spectral resolution enables measurements in the red and NIR of strong absorption features, especially those needed for fluorescence line height and atmospheric correction. However, the main advantages are found in the application. The WISP-3 is the most easy to handle instrument: the sensors are set in the correct angles, no cables, laptop computer or electricity are needed in the field and by just one press on the button, five measurements are taken, averaged, and saved. Therefore, less experienced samplers would be able to perform measurements with a similar accuracy.

With the results of the current assessment it can be stated that with the WISP-3 radiometer, reflection spectra can be obtained with accuracies in the same range as well-known instruments, although the calibration can be improved with implementing a calibration with an NIST traceable calibration setup.

Simple band algorithms can be programmed into the WISP-3 and used to derive water quality parameters (Chl, SPM, aCDOM). These algorithms need regional tuning. In the analysis, the band ratios proposed for Chl and SPM retrieval in Lake Vänern also worked for Lake Peipsi, showing strong correlations between the ratio and the *in situ* measured concentration. For CDOM, the ratio only showed a strong correlation for the Lake Vänern stations. For Lake Peipsi another algorithm or another tuning would be required. It can be concluded that with a suitable regional algorithm, the WISP-3 can be used for fast water quality assessments of Chl and SPM

concentrations for routine monitoring. It can also be used by remote sensing experts to obtain reflection spectra from water bodies for remote sensing purposes.

Acknowledgments

Niklas Strömbeck is thanked for his help in organizing the field campaign and performing the Microtops measurements. Evi Lill of the Centre for Limnology of Estonian University of Life Sciences is thanked for performing the laboratory measurements of Lake Peipsi. This project has been funded by EU FP7 PEOPLE project WaterS, and partly by the projects CYAN-IS-WAS (Science and technological cooperation between Italy and the Kingdom of Sweden, MIUR), the European Space Agency ESA (contract 21524/08/1-OL) and the Swedish National Space Board.

References

1. I. S. Robinson et al., "Remote sensing of shelf sea ecosystems: state of the art and perspectives," *ESF Marine Board Position Paper*, **12**, European Science Foundation, ESF Marine Board, Ostend, Belgium (2008).
2. M. Bresciani et al., "Assessing remotely sensed chlorophyll-*a* for the implementation of the Water Framework Directive in European perialpine lakes," *Sci. Total Environ.* **409**(7), 3083–3091 (2011), http://dx.doi.org/10.1016/j.scitotenv.2011.05.001.
3. S. Kratzer, C. Brockmann, and G. Moore, "Using MERIS full resolution data to monitor coastal waters—A case study from Himmerfjärden, a fjord-like bay in the northwestern Baltic Sea," *Rem. Sens. Environ.* **112**(5), 2284–2300 (2008), http://dx.doi.org/10.1016/j.rse.2007.10.006.
4. A. Reinart and K. Valdmets, "Variability of optical water types in Lake Peipsi," *Proc. Estonian Acad. Sci. Biol. Ecol.* **56**(4), 33–46 (2007).
5. L. Guanter et al., "Atmospheric correction of ENVISAT/MERIS data over inland waters: validation for European lakes," *Rem. Sens. Environ.* **114**(5), 467–480 (2010), http://dx.doi.org/10.1016/j.rse.2009.10.004.
6. C. Hu, "Simple instrument for measurement of remote sensing reflectance in coastal environment," *Proc. SPIE* **4897**, 219–226 (2002), http://dx.doi.org/10.1117/12.467402.
7. C. D. Mobley, "Estimation of the remote-sensing reflectance from above-surface measurements," *Appl. Opt.* **38**(36), 7442–7455 (1999), http://dx.doi.org/10.1364/AO.38.007442.
8. H. J. Gons, M. Rijkeboer, and K. G. Ruddick, "Effect of a waveband shift on chlorophyll retrieval from MERIS imagery of inland and coastal waters," *J. Plankton Res.* **27**(1), 125–127 (2005), http://dx.doi.org/10.1093/plankt/fbh151.
9. S. Simis, "Blue-green catastrophe: remote sensing of mass viral lysis of cyanobacteria," Ph.D. Thesis, Vrije University, Amsterdam (2006).
10. M. Rijkeboer, "Algoritmen voor het bepalen van de concentratie chlropfyl-a and zwevend stof met de Optische Teledetectie Methode in verschillende optische watertypen," Insituut voor Milieuvraagstukken, Amsterdam, The Netherlands (2000).
11. H. J. Van Der Woerd and R. Pasterkamp, "HYDROPT: a fast and flexible method to retrieve chlorophyll-*a* from multispectral satellite observations of optically complex coastal waters," *Rem. Sens. Environ.* **112**(4), 1795–1807 (2008), http://dx.doi.org/10.1016/j.rse.2007.09.001.
12. G. P. Eppeldauer, S. W. Brown, and K. R. Lykke, "Transfer standard filter radiometers: applications to fundamental scales," in *Optical Radiometry. Experimental Methods in the Physical Sciences*, A. Parr, R. Datla, and J. Gardner, Eds, Vol. **41**, pp. 51–211, Elsevier Academic Publishers, San Diego (2005).
13. K. Ruddick, V. De Cauwer, and B. Van Mol, "Use of the near infrared similarity reflectance spectrum for the quality control of remote sensing data," *Proc. SPIE* **5885**, 588501 (2005), http://dx.doi.org/10.1117/12.615152.
14. K. Ruddick et al., "Seaborne measurements of near infrared water-leaving reflectance: the similarity spectrum for turbid waters," *Limnol. Oceanogr.* **51**(5), 1167–1179 (2006), http://dx.doi.org/10.4319/lo.2006.51.2.1167.

15. G. Zibordi et al., "AERONET-OC: an overview," *Can. J. Rem. Sens.* **36**(5), 488–497 (2010), http://dx.doi.org/10.5589/m10-073.
16. IOCCG, "Remote sensing of ocean colour in coastal, and other optically-complex, waters," in *Reports of the International Ocean-Colour Coordinating Group, No. 3*, S.Sathyendranath, Ed., IOCCG, Dartmouth, Canada (2000).
17. G. Zibordi et al., "*In situ* determination of the remote sensing reflectance: an inter-comparison," *Ocean Sci. Discuss.* **9**, 787–833 (2012), http://dx.doi.org/10.5194/osd-9-787-2012.
18. K. Barker, "MERIS optical measurement protocols," Part A: *Reflectance*, Issue 2.0 Rev.1.0. Doc. no: CO-SCI-ARG-TN-0008, ARGANS Ltd., p. 133, (2011), http://hermes.acri.fr/mermaid/dataproto/CO-SCI-ARG-TN-0008_MERIS_Optical_Measurement_Protocols_Issue2_Aug2011.pdf (7 December 2012).
19. WetLabs, "Ac-meter protocol" Revision Q, (2011), http://www.wetlabs.com/sites/all/modules/pubdlcnt/pubdlcnt.php?file=http://www.wetlabs.com/sites/default/files/documents/acprotq.pdf&nid=625 (7 December 2012).
20. J. T. O. Kirk, *Light and Photosynthesis in Aquatic Ecosystems*, 2nd ed., Cambridge University Press, Cambridge, United Kingdom (1994).
21. J. L. Mueller, G. S. Fargion, and C. R. McClain, "Ocean optics protocols for satellite ocean color sensor validation," Revision 4, Vol. I-VII, NASA, Goddard Space Flight Space Center, Greenbelt, Maryland (2003).
22. R. E. Bird and C. J. Riordan, "Simple solar spectral model for direct and diffuse irradiance on horizontal and tilted planes at the earth's surface for cloudless atmospheres," *J. Clim. Appl. Meteorol.* **25**(1), 87–97 (1986), http://dx.doi.org/10.1175/1520-0450(1986)025<0087:SSSMFD>2.0.CO;2.
23. G. Thuillier et al., "The solar spectral irradiance from 200 to 2400 nm as measured by the SOLSPEC spectrometer from the ATLAS 1-2-3 and EURECA missions," *Sol. Phys.* **214**(1), 1–22 (2003), http://dx.doi.org/10.1023/A:1024048429145.
24. G. Zibordi et al., "An autonomous above-water system for the validation of ocean color radiance data," *IEEE Trans. Geosci. Rem. Sens.* **42**(2), 401–415 (2004), http://dx.doi.org/10.1109/TGRS.2003.821064.
25. D. P. Pierson and N. Strömbeck, "A modeling approach to evaluate preliminary remote sensing algorithms: use of water quality data from Swedish great lakes," *Geophysica* **36**(1–2), 177–202 (2000).
26. A. Hommersom et al., "Spatial and temporal variability in bio-optical properties of the Wadden Sea," *Est. Coast. Shelf Sci.* **83**(3), 360–370 (2009), http://dx.doi.org/10.1016/j.ecss.2009.03.042.
27. J. N. Porter et al., "Ship-based sun photometer measurements using Microtops sun photometers," *J. Atm. Ocean. Tech.* **18**(5), 765 (2001), http://dx.doi.org/10.1175/1520-0426(2001)018<0765:SBSPMU>2.0.CO;2.
28. M. Doron et al., "Spectral variations in the near-infrared ocean reflectance," *Rem. Sens. Env.* **115**(7), 1617–1631 (2011), http://dx.doi.org/10.1016/j.rse.2011.01.015.
29. M. Babin et al., "Variations in the light absorption coefficients of phytoplankton, nonalgal particles, and dissolved organic matter in coastal waters around Europe," *J. Geophys. Res.-Ocean.* **108**(3211), 1–20 (2003), http://dx.doi.org/10.1029/2001JC000882.

Biographies and photographs of the authors are not available.